© 2018 IEEE. Personal use of this material is permitted. Permission from IEEE must be obtained for all other uses, including reprinting/republishing this material for advertising or promotional purposes, collecting new collected works for resale or redistribution to servers or lists, or reuse of any copyrighted component of this work in other works.

User Force-Dependent Variable Impedance Control in Human-Robot Interaction

Florian Müller, Jan Janetzky, Uwe Behrnd, Jens Jäkel and Ulrike Thomas

***Abstract*— In this paper a novel type of variable impedance control (VIC) is presented. The controller adjusts the impedance depending on the force input of the user. In this way it is easy to accelerate and decelerate. Additionally, for high velocity the damping decreases and vice versa. This approach could be interpreted as a combination of acceleration-dependent VIC and velocity-dependent VIC. To guarantee stability, a stability observer is introduced. The observer is based on a model which describes a combined passive and active behavior of the user. In addition, we present a user study with 45 participants where the differences between VIC, VIC with stability observer and a pure admittance controller were investigated. The results show an improvement of the VIC with stability observer in relation to the pure admittance controller among different categories. With both the variable impedance controller and the variable impedance controller with stability observer, the participants significantly improved their times in comparison to the pure admittance controller, while they maintained the same level of precision. Also the workload was considerably smaller and the user comfort increased with both controllers compared to the usage of the pure admittance controller.**

I. Introduction

The latest trend in physical human-robot interaction (pHRI) is shaped by a shift towards industrial environments and away from laboratories in enabled by modern safety technology standards. The pHRI is an answer to a claim for more flexibility needed in industrial processes. Fields of applications are lifting heavy workpieces with a hand-guided robot, teaching robots or collaborative assembly tasks. The technological contemplation is based on sensing user applied forces and an impedance or admittance controller.

The general approach of impedance control is based on Hogan [14]. This concept was designed for all kinds of contacts between robots and their environment. To adapt the impedance controller to the context of a physical human-robot interaction Ikeura and Inooka introduced the variable impedance control (VIC) [15]. These authors discovered that the stiffness of the arm muscles is higher in positioning tasks than in tasks with rapid motions. Therefore, they proposed an impedance controller with velocity-dependent damping. For a low velocity the damping is high and vice versa. Several authors developed the this idea of a variable impedance controller. One thing that all these concepts have in common is that one or more impedance parameters depend on time-variant environmental parameters. In the present paper the term *variable impedance control* is also used for similar concepts with an admittance controller.

A concept which also uses a velocity-dependent VIC with an exponential characteristic was presented in [10]. In this concept and in addition to the variable damping the mass parameter is also variable in order to guarantee the stability of the system. Use cases for the velocity-dependent VIC can be found in robot assisted welding [9], [8].

Another approach is to design the VIC with a dependence on human arm stiffness [25]. The authors estimate the stiffness online with the ratio between the derivative of the user force and the derivative of the position. With peg-in-hole experiments the authors show the effectiveness of this method for positioning tasks [26]. A similar approach is presented in [12], where the authors measured the stiffness indirectly by the muscle activity with electromyography instead of estimating the stiffness. However, in their user study the authors could not indicate any improvement with their approach. Furthermore, in [29] another stiffness based VIC is presented.

A further VIC approach was introduced by Duchaine and Gosselin [6]. Their approach is based on the idea of identifying the human intention of acceleration and deceleration and to adapt the damping accordingly. This is realized by using the derivative of the force filtered by a low-pass. In user studies [5], [4] the authors show an obvious improvement with their approach. The participants had a lower error rate and needed less time. In [18] the authors describe an approach with a direct dependence on acceleration.

Further possibilities for the realization of VIC includes the potential force field-dependent VIC [21], the user force and velocity-dependent VIC using fuzzy logic based adaptation [3] and task specific VIC [30] which is based on learning data.

Due to reasons of varying impedance parameters an online stability observation is necessary. In [10] and [27] the authors use numerical approaches based on experimental data with their robots. In contrast Duchaine and Gosselin developed an analytical stability observer for their VIC based on the Lyapunov method [7]. Due to their unconventional use of a low-pass filter in front of the impedance controller, this stability observer is unsuitable for other VIC methods. A conservative method to guarantee stability is Colgate's Passivity condition [2]. In [20] a stability analysis for pHRI with a human model which includes a response time was presented. The stability proof is based on the Lyapunov-Krasovskii functional. The

Florian Müller and Ulrike Thomas are with the Chair of Robotics and Human-Machine-Interaction Lab, Chemnitz University of Technology, Email: florian.mueller@etit.tu-chemnitz.de, ulrike.thomas@etit.tu-chemnitz.de

Jan Janetzky, Uwe Behrnd and Jens Jäkel are with the Department Electrical Engineering and Information Technology, Leipzig University of Applied Sciences, Email: jan.janetzky@stud.htwk-leipzig.de, uwe.behrnd@stud.htwk-leipzig.de, jens.jaekel@htwk-leipzig.de

concept was extended for a more detailed human model in [19].

Inspired by the ideas of velocity and acceleration dependent VIC we present in this paper the user force dependent VIC. From the authors' point of view, this concept is a combination of the velocity and acceleration dependent VIC and combines their advantages. Furthermore, we derive a stability observer based on the stability criterion of [19] in order to guarantee stable behavior.

In this paper, we investigate different aspects of the presented controller types in a user study, e.g. workload and user comfort. The perceived workload is a multidimensional approach in order to measure how demanding a task is under specific conditions or how many resources are required for a certain task performance, see [13]. User comfort is a pleasant reaction to the environment. It is influenced by the physical and physiological perceptions of the used product and the task, such as posture and applied force, as well as their subjective interpretations, see [28]. Both aspects allow insights into the comfort of the task and tool.

The paper is structured as follows: In Sec. II we focus on the description of Cartesian admittance control and introduce the user force-dependent VIC approach. In Sec. III the stability observer with the underlying human model and the stability criterion is derived. The user study which investigates the improvement of the user force-dependent VIC is described in Sec. IV. The corresponding results are disused in Sec. V. The paper is concluded in Sec. VI and gives an outlook.

II. Impedance Control

A. Cartesian Admittance Control

The use of an admittance controller is recommended when no dynamic model of the robot is available. The forces and torques applied by the user on the end-effector are measured by a force/torque sensor with six degree of freedom at the end-effector. The Cartesian admittance controller is described by the desired dynamic behavior of the end-effector

$$\boldsymbol{M}\ddot{\boldsymbol{x}} + \boldsymbol{D}\dot{\boldsymbol{x}} = \boldsymbol{\Gamma}. \tag{1}$$

with the admittance parameters for mass $\boldsymbol{M} \in \mathbb{R}^{6\times6}$ and for damping $\boldsymbol{D} \in \mathbb{R}^{6\times6}$, the position and orientation (pose) of the end-effector $\boldsymbol{x} = [\boldsymbol{p}^T, \boldsymbol{\omega}^T]^T \in \mathbb{R}^6$ and the vector with the measured forces and torques at the end-effector $\boldsymbol{\Gamma} = [\boldsymbol{F}^T, \boldsymbol{\tau}^T]^T \in \mathbb{R}^6$. The admittance parameters $\boldsymbol{M}$ and $\boldsymbol{D}$ are diagonal matrices, whereby $\boldsymbol{D}$ in this paper is a time-variant variable for the VIC, see Sec. II-B.

For the implementation of this behavior in a robot with an arbitrary number of n joints, the velocity of the joint angles $\dot{\boldsymbol{q}} \in \mathbb{R}^n$ can be calculated using the pseudo inverse Jacobian matrix $\boldsymbol{J}^+ \in \mathbb{R}^{n\times6}$ in

$$\dot{\boldsymbol{q}} = \boldsymbol{J}^+\dot{\boldsymbol{x}}. \tag{2}$$

To apply this concept the robot needs to be velocity controlled.

In the context of the following introduction of VIC the admittance control will be denoted as pure admittance control (PAC) in the following sections.

B. Force-Dependent Variable Impedance Control

The idea behind a user force-dependent variable impedance control is the following:

- In the steady state of the impedance controller, the velocity is proportional to the input force. For this reason a velocity-dependent VIC as in [15] and [10] is in a steady state similar to a force-dependent VIC.
- During an acceleration or deceleration phase the input force is nearly proportional to the acceleration. Therefore, the user force-dependent VIC is a form of combination of velocity and acceleration based VIC.

From this we deduce the following control law of the variable impedance controller:

$$\boldsymbol{D}(\boldsymbol{\Gamma}) = -\alpha\,\mathrm{diag}(\boldsymbol{\Gamma})\,\mathrm{diag}(\mathrm{sgn}(\dot{\boldsymbol{x}})) + \boldsymbol{D}_0 \tag{3}$$

with the constant parameter diagonal matrix $\boldsymbol{D}_0 \in \mathbb{R}^{6\times6}$ for the damping values, the signum function $\mathrm{sgn}()$ and the tuning parameter $\alpha \in \mathbb{R}^+$. With the sign-function the damping decreases if the force and the velocity have the same direction. Otherwise the damping increases. More precisely, during the acceleration of the end effector the damping decreases and vice versa. Thus, the control law enhances these processes. Additionally, when the force and thus the velocity are constant, the damping decreases too and supports the user intended motion.

For an illustration of these effects, Fig. 1 shows an example with an acceleration and a deceleration phase in a certain direction followed by a phase of constant force. During the first two seconds the figure shows the acceleration and deceleration phases. After $5\,\mathrm{s}$ a phase of constant force and velocity occurs. Due to the user force-dependent VIC the damping parameter changes as shown.

III. Stability

A. Human model

For the derivation of a stability observer we consider the one-dimensional pHRI system including an impedance controller and a linear virtual environment, see Fig. 2 for the corresponding block diagram. This system is a modification of the pHRI model of [19]. The impedance controller includes a virtual mass m_i and a virtual damping d_i. The particular aspect of the human model is the consideration of a combined passive and active human behavior including a response time τ. This model is also shown in Fig. 2.

The passive part considers the classic human model with the mass of the human arm m_H and its damping d_H. Opposing the common assumption, this model includes no passive stiffness. Passive stiffness of the human arm can only occur in the immediate vicinity of hinge stops. Such circumstances will not be considered.

The active part describes all active reactions of the human affected by the central nervous system. This includes the

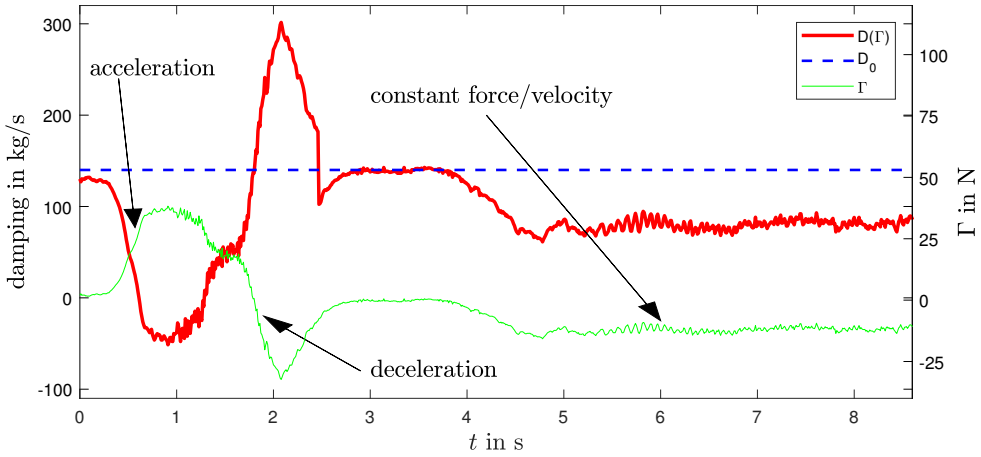


Fig. 1. Example of acceleration and deceleration with a subsequent phase of constant force showing the progression of the variable damping in one dimension (D – damping computed by the variable impedance controller, D_0 – constant damping, Γ – user forces/torques).

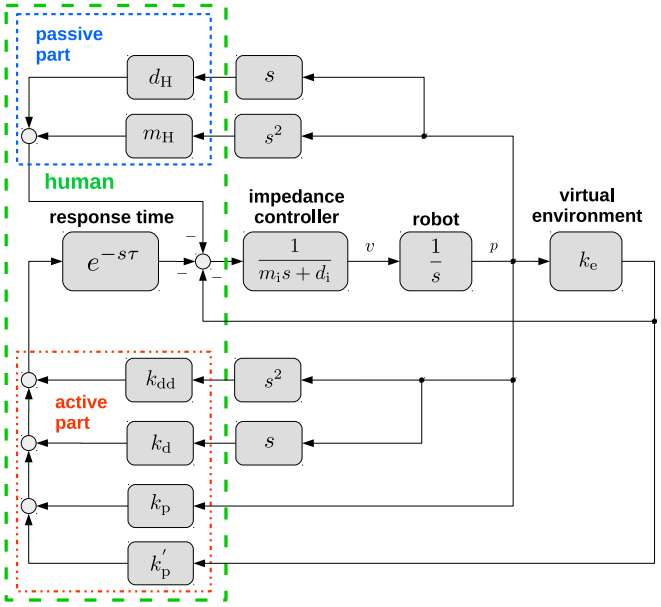


Fig. 2. Block diagram of a pHRI system with human model consisting of a passive part and an active part.

reaction on acceleration, velocity, position and force. The force is represented through a linear virtual environment k_e. Such a virtual environment is used for avoiding limit stops or for avoiding collisions with obstacles. The reaction to the force is described by the gain $k_\mathrm{p}^{'}$, the reaction to the position by the gain k_p and the reaction to the velocity by the gain k_d. The behavior could be described as a delayed PDD^2-controller. The D^2-term k_dd reacts to the system acceleration. All these reactions are affected by a response time τ. A common application for this term is the delayed resonator for vibration absorption [22].

This description results in a two-dimensional state space model

$$\begin{aligned}\dot{v} &= -\frac{d}{m}v - \frac{k_\mathrm{e}}{m}p - \frac{k_\mathrm{d}}{m}v(t-\tau) - \frac{k_\mathrm{p}+k_\mathrm{p}^{'}k_\mathrm{e}}{m}p(t-\tau) \\ &\quad - \frac{k_\mathrm{dd}}{m}\dot{v}(t-\tau) \\ \dot{p} &= v \end{aligned} \tag{4}$$

with the overall mass, damping and active stiffness

$$m = m_\mathrm{i} + m_\mathrm{H}, \tag{5}$$
$$d = d_\mathrm{i} + d_\mathrm{H}. \tag{6}$$

For the stability proof the approximated matrix form of (4) is used:

$$\begin{aligned}\begin{bmatrix}\dot{v}\\ \dot{p}\end{bmatrix} &= \begin{pmatrix}-\frac{d}{m} & -\frac{k_\mathrm{e}}{m}\\ 1 & 0\end{pmatrix}\begin{bmatrix}v\\ p\end{bmatrix} + \sum_{i=1}^{N^*}\left(-\frac{k_\mathrm{dd}}{m}\right)^i \\ &\quad \cdot \begin{pmatrix}\frac{k_\mathrm{d}}{k_\mathrm{dd}} - \frac{d}{m} & \frac{k_\mathrm{p}+k_\mathrm{p}^{'}k_\mathrm{e}}{k_\mathrm{dd}}\\ 0 & 0\end{pmatrix}\begin{bmatrix}v\\ p\end{bmatrix}(t-i\tau)\,. \end{aligned} \tag{7}$$

N^* is calculated with

$$\sum_{i=1}^{N^*}\left(-\frac{k_\mathrm{dd}}{m}\right)^i > \frac{W}{100\%}\frac{-k_\mathrm{dd}}{(k_\mathrm{dd}+m)}. \tag{8}$$

where W is the percentage accuracy for model approximation. Further details to be found in [19].

The state space model for a robot with $n \geq 6$ has six degrees of freedom (dof) in Cartesian space which results in a twelve dimensional state space model. We assume the dof are approximately decoupled. Then (4) can be applied separately to each degree of freedom of the robotic system.

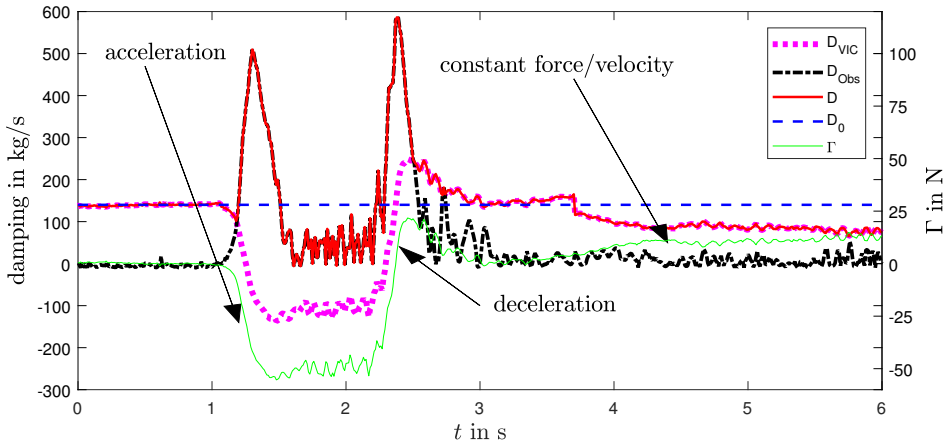


Fig. 3. Block diagram of a pHRI system with human model consisting of a passive part and an active part (D_{VIC} – damping computed by the variable impedance controller, D_{Obs} – lowest damping computed by the stability observer, D – combination of D_{Obs} and D_{VIC}, D_0 – constant damping, Γ – user forces/torques).

B. Stability Law

From [19] we know that (7) is asymptotically stable if the conditions

$$d > \frac{\pm k_{\text{d}} + \left| k_{\text{p}} + k_{\text{p}}^{'} k_{\text{e}} - k_{\text{e}} \frac{k_{\text{dd}}}{m} \right| \tau \frac{\sqrt{\left(\frac{k_{\text{dd}}}{m}\right)^2 + 1}}{1 - \left(\frac{k_{\text{dd}}}{m}\right)^2}}{\sqrt{\frac{1 - \left(\frac{k_{\text{dd}}}{m}\right)^2}{N^*}} \pm \frac{k_{\text{dd}}}{m}} \tag{9}$$

$$0 < k_{\text{p}} + k_{\text{p}}^{'} k_{\text{e}} + k_{\text{e}} \tag{10}$$

are fulfilled. For a stability observer we assume all these parameters are fixed, with exception of the active damping k_{d} and the active stiffness k_{p}.

This stability law is used for checking every component of $\boldsymbol{D}(\boldsymbol{\Gamma}) = \text{diag}\,(D_1,\ D_2, ..., D_6)$ in order to guarantee that all D_i are higher than the right-hand side of (9). The parameters used in (9) could vary for every component of $\boldsymbol{D}$.

C. Estimation of Active Damping and Stiffness

The active damping and stiffness will be estimated by a modification of the approach of [25]. For the active stiffness the ratio of the derivative of user force and the derivative of the velocity is used:

$$k_{\text{p}} = \frac{\dot{\Gamma}}{\dot{p}}. \tag{11}$$

This means that the muscular activity is high when the force is changing and the velocity is low. A similar approach is applied for the active damping

$$k_{\text{d}} = \frac{\dot{\Gamma}}{\dot{v}}. \tag{12}$$

instead of the derivative of the position, the derivative of the velocity is used. In order to avoid large steps in the resulting signal $\dot{\Gamma}$, $\dot{p}$ and $\dot{v}$ are filtered by a low-pass filter with a small time constant T.

This approach could be interpreted as an additional combination of the user force-dependent VIC with a stiffness-dependent VIC. This means the VIC with stability observer (Obs.) combines three of the established VIC approaches.

D. Functional Principle of the Stability Observer

In order to demonstrate the functional principle of the stability observer in combination with the user force-dependent VIC an acceleration and deceleration in x-direction is considered. Fig. 3 shows an example. The VIC controller D_{VIC} is defined by (3) and the stability observer by (9). The damping D is the maximum of D_{VIC} and D_{Obs} ($D = \max\{D_{\text{VIC}}, D_{\text{Obs}}\}$). For an acceleration process the damping of the VIC controller D_{VIC} is strongly decreased in contrast to the damping calculated by the stability observer D_{Obs}, which has an visible increase. Immediately after the acceleration the damping D decreases due to the damping of the stability observer. Furthermore, D_{VIC} and D_{Obs} increase for the deceleration process. However, in this case D_{Obs} is obviously more dominant, which results in $D = D_{\text{Obs}}$. From second 4 to second 6 the user applied a constant force. This has the effect of a proportional decrease in damping $D = D_{\text{VIC}}$ in relation to the user force Γ.

The figure show that $D_{\text{Obs.}}$ defines often the lower limit of D to avoid the usage of the potentially unstable values of D_{VIC}. This guarantees the stability of the controller.

IV. User Study

With the experiment described below we investigated whether there are differences between the VIC with stability observer (in the following VIC+Obs.) and the PAC and also between the VIC and the PAC regarding the number of errors, the experimental runtime, workload and user comfort.

A. Hypotheses

Our hypotheses are that both types of the VIC have a significant difference in the experimental runtime and no significant differences in the number of errors. We conclude this

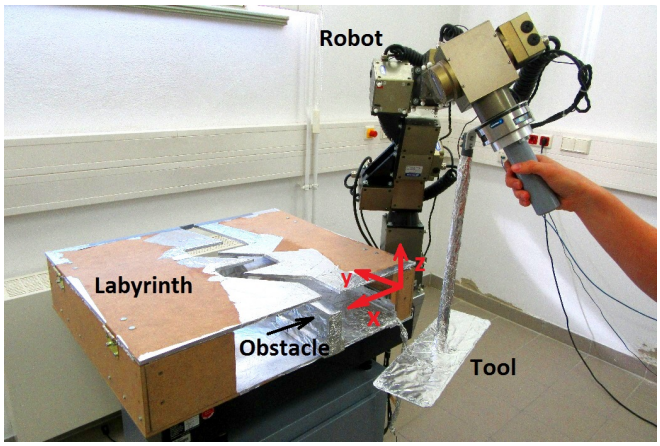


Fig. 4. Test bed: the base coordinate system (red) is located in the center of the robot base.

hypothesis from the results of the user studies of [18], [10]. As a result, we assume a lower experimental runtime for the VIC+Obs. in comparison to the VIC because the VIC+Obs. includes higher damping values. By comparing the norm of the user forces and torques averaged over time we expect the highest forces/toques for PAC, followed by VIC+Obs. and the lowest forces/toques for VIC. Furthermore, we assume significant differences for the workload and different aspects of user comfort by comparing the two types of VIC with the PAC. We expect that the VIC+Obs. has the best workload and user comfort due to the stability observer stabilizing the whole system.

B. Test bed and parameters

The test bed consists of a six dof robotic arm with a tool fixed to the end effector, see Fig. 4. The robot arm consists of SCHUNK PowerCubes. The picture shows how the user guides the robot with the tool through a simple labyrinth. In order to increase the difficulty of the task, two obstacles were placed in the labyrinth. In order to avoid contact between the tool and the labyrinth, the user has to hold the appropriate pose of the robotic arm during the guiding process. The user has to grasp the handle at the tip of the robot. The width of the labyrinth's path has a range between $0.055\,\mathrm{m} - 0.065\,\mathrm{m}$ and the length of the path is about $1.00\,\mathrm{m}$. The labyrinth has a height of $0.14\,\mathrm{m}$. The tool consists of a shaft and a tray. The shaft has a length of $0.43\,\mathrm{m}$ and a diameter of $0.02\,\mathrm{m}$ and the tray has the dimensions $0.38\,\mathrm{m}$ x $0.11\,\mathrm{m}$. The angle between tool and handle is $30°$. For safety reasons an enabling switch is mounted to the handle.

The chosen start position of the robot is $\boldsymbol{x}_\mathrm{s} = [-0.5\,\mathrm{m}\ \ 0\,\mathrm{m}\ \ 0\,\mathrm{m}\ \ 145°\ \ 0°\ \ 90°]^T$ in relation to the base coordinate system, see Fig. 4. This results in the user task of bringing the tool to the right pose before the user can cross the labyrinth. The impedance controller is parametrized with $\boldsymbol{M} = \mathrm{diag}(100\,\mathrm{kg}\ \ 100\,\mathrm{kg}\ \ 100\,\mathrm{kg}\ \ 5\,\mathrm{kgm}^2\ \ 5\,\mathrm{kgm}^2\ \ 5\,\mathrm{kgm}^2)$ and $\boldsymbol{D} = \boldsymbol{D}_0 = \mathrm{diag}(140\,\mathrm{kg/s}\ \ 140\,\mathrm{kg/s}\ \ 140\,\mathrm{kg/s}\ \ 14\,\mathrm{kgm}^2/\mathrm{s}\ \ 14\,\mathrm{kgm}^2/\mathrm{s}\ \ 14\,\mathrm{kgm}^2/\mathrm{s})$.

The tuning parameter of the VIC is set to $\alpha = 5$. This setting is the result of empirical tests and $\alpha = 5$ was chosen to guarantee that the user will take notice of the effect of the VIC. For the stability observer the passive human parameters will be assumed as $m_\mathrm{H} = 1\,\mathrm{kg}$, $d_\mathrm{H} = 10\,\mathrm{kg/s}$ which is orientated on the table of [11, p. 4]. For the parameters of the active part of human model we use the assumptions $k_\mathrm{dd} = 0.1\,\mathrm{kg}$, $k_\mathrm{p}^{'} = 0.5\,\mathrm{kg/s^2}$. For the human response time we chose $\tau = 150\,\mathrm{ms}$ as an empirical value. The model accuracy is set to $W = 98\,\%$. To avoid extremely high values for the active damping and the active stiffness minimum values $\dot{p}_\mathrm{min} = [0.4\,\mathrm{m/s}\ \ 0.4\,\mathrm{m/s}\ \ 0.4\,\mathrm{m/s}\ \ 40\,°/\mathrm{s}\ \ 40\,°/\mathrm{s}\ \ 40\,°/\mathrm{s}]^T$ and $\dot{v}_\mathrm{min} = [0.4\,\mathrm{m/s^2}\ \ 0.4\,\mathrm{m/s^2}\ \ 0.4\,\mathrm{m/s^2}\ \ 40\,°/\mathrm{s^2}\ \ 40\,°/\mathrm{s^2}\ \ 40\,°/\mathrm{s^2}]^T$ are assigned. The time constant of the low-pass filter is set to $T = 100\,\mathrm{ms}$.

In order to avoid reaching joint limits every joint has a linear virtual stiffness $\boldsymbol{k}_\mathrm{e}^q$ close to the corresponding lower $\boldsymbol{q}_i^-$ and upper joint limits $\boldsymbol{q}_i^+$. With the safety distance $\boldsymbol{q}_i^\mathrm{sd}$ we obtain the torques

$$\boldsymbol{\tau}_+ = \mathrm{diag}(\boldsymbol{k}_\mathrm{e}^q)\left(\boldsymbol{q} - \boldsymbol{q}^+ + \boldsymbol{q}^\mathrm{sd}\right), \quad \text{for} \quad \boldsymbol{q} > \boldsymbol{q}^+ - \boldsymbol{q}^\mathrm{sd} \tag{13}$$

$$\boldsymbol{\tau}_- = \mathrm{diag}(\boldsymbol{k}_\mathrm{e}^q)\left(-\boldsymbol{q} + \boldsymbol{q}^+ + \boldsymbol{q}^\mathrm{sd}\right), \quad \text{for} \quad \boldsymbol{q} < \boldsymbol{q}^- + \boldsymbol{q}^\mathrm{sd}. \tag{14}$$

In any other case $\boldsymbol{\tau}_+ = 0$ and $\boldsymbol{\tau}_- = 0$. For the transfer into Cartesian space

$$\boldsymbol{\Gamma}_{q^+} = -\left({\boldsymbol{\tau}_+}^T \boldsymbol{J}^{+^{-1}}\right)^T \text{ and } \boldsymbol{\Gamma}_{q^-} = -\left({\boldsymbol{\tau}_-}^T \boldsymbol{J}^{+^{-1}}\right)^T \tag{15}$$

are used. Finally, $\boldsymbol{\Gamma}_{q^+}$ an $\boldsymbol{\Gamma}_{q^-}$ are added to the right-hand side of (1). The stiffness of the virtual environment for the stability observer is calculated by using

$$\boldsymbol{k}_\mathrm{e} = \frac{\boldsymbol{\Gamma}_{q^+}}{\boldsymbol{q} - \boldsymbol{q}^+ + \boldsymbol{q}^\mathrm{sd}} + \frac{\boldsymbol{\Gamma}_{q^-}}{-\boldsymbol{q} - \boldsymbol{q}^+ + \boldsymbol{q}^\mathrm{sd}}. \tag{16}$$

The parametrization for the joint limit avoidance is $\boldsymbol{k}_\mathrm{e}^q = [4\ 1.4\ 1.2\ 1.1\ 1\ 0.8]^T\mathrm{Nm}/°$, $\boldsymbol{q}^- = [-153°\ -95°\ 20°\ -120°\ 25°\ -170°]^T$ and $\boldsymbol{q}^+ = [153°\ 95°\ 120°\ 120°\ 125°\ 170°]^T$.

C. Participants

Forty-five participants mostly students and employees of the Leipzig University of Applied Science and of the University of Leipzig (31 male, 14 female, age: mean = 27.1 years, standard deviation = 7.3 years, range: 15 – 51) were recruited. The participants were randomly assigned to three equally sized groups which are differentiated by the sequences of settings (VIC, PAC, VIC+Obs.). For group A the sequence is *VIC, PAC, VIC+Obs.*, for group B *VIC+Obs., VIC, PAC*, for group C *PAC, VIC+Obs., VIC*. This procedure is used to take into account learning effects of the participants. All participants were rewarded for their contribution to the user study. To instill motivation for passing the test bed as quickly as possible and with a minimal number of errors the study was organized as a competition. All participants were informed that every error leads to time penalty of 10 s. The participant with the lowest total time was rewarded.

D. Design and Procedure

The user study had a mixed design (within and between participants). All participants conducted three trials, one trial with VIC, one with PAC and one with VIC+Obs (within participants). The sequence of trials with VIC, PAC and VIC+Obs. was varied between group A, B and C (between participants).

In every trial the participants cross the labyrinth and return to the start. Before starting the regular three trials, the participants were instructed to carry out one test run with the setting PAC. The advantage of this is a reduction of the learning effects during the regular three trials. In the following three trials with the group-dependent setting were completed and after every trial the participants were asked to fill out a questionnaire. Additionally, a final questionnaire was completed. The participants did not know in which order the setting would occur.

The trial performance was measured by the time needed to guide the tool through the labyrinth of the test bed using the robot. The number of contacts between the tool and the test bed were recorded too. A trial started with the first push on the enabling switch and ended with the final release of the enabling switch. Every contact between the tool and the test bed generated an acoustic signal and added to an error counter. The counter rated multiple contacts in a time period of $0.3\,\mathrm{s}$ for one error and for permanent contacts every $1.5\,\mathrm{s}$ an additional error. Also the user forces and torques were measured every $10\,\mathrm{ms}$.

E. Questionnaire

The questionnaire consisted of questions from the Comfort Questionnaire for Handtools (CQH), see [17], which was selected to rate the comfort of the hand-guided robot. An adapted version of the CQH was used to avoid neutral ratings (1 – 2: unsatisfied, 3 – 4: satisfied somewhat, 5 – 6: fully satisfied), see [16] and also Table I no. 6 – no. 10. The comfort rating was complemented with our own questions regarding task and robot characteristics, see Table I no. 11 – no. 15.

Additionally, the subjective workload of each task was assessed within the dimensions of mental, physical, and temporal demand, perceived performance, effort as well as stress and frustration, see [13]. It was measured by the NASA Raw Task Load Index, see [1]. The NASA TLX is a widely accepted and applied instrument in Human Factors, see [13].

Finally, a last questionnaire with four questions was designed. In the first three questions the participants were asked: Which trial was better? (no.1: trial 1 or trial 2, no. 2: trial 2 or trial 3, no. 3: trial 2 or trial 3) on a scale from 1 to 6. The final question (no. 4) was: Which trial was the best? The answer should be trial 1, 2 or 3 and was not represented by a scale.

V. Results and Discussion

The resulting data were sorted considering their group-dependent sequence into the three categories: VIC, VIC+Obs. and PAC. With the paired t-test [24, p. 266 ff.] our initial hypotheses were tested on significances. This means the t-test was applied between VIC+Obs. and PAC and between VIC and PAC. The t-test requires a normal distribution which is not satisfied for our data. However, for a large sample size ($n > 30$) the t-test is robust to violations of the normality requirement [23, p. 359]. Table I shows the results of the user study. The columns with $|t(0.975, n\text{-}1)|$ contain the absolute values of the results from the t-test with a $5\,\%$ level and the sample size n. The sample size varies because in the case of line no. 3 and line no. 4 some data recording failed and in the other cases some participants missed some questions in the questionnaires. The p value measures significance and is the result of the t-test. With a p value smaller than 0.05 we consider a difference as significant (marked in bold). For $0.05 < p < 0.1$ the difference is statistically not significant, but there is a weak evidence (marked in italic). The columns with VIC+Obs., PAC and VIC contain the mean value μ and the corresponding standard deviation σ.

According to our hypothesis we found no significant difference between the number of errors of VIC+Obs. and VIC to PAC (Table I, line no. 1). This corresponds to the subjective experience of the participants given by the answers (Table I, line no. 11), where the participants were asked for the precision of the robot.

Confirming our hypothesis, the VIC+Obs. reduces the experimental runtime (Table I, line no. 2). There is an improvement of $7\,\%$ which is a similar to [10]. However, the results between PAC and VIC shows no significant difference which refutes our hypothesis. For a difference between VIC and VIC+Obs. the data shows only a weak evidence .

The high value of the σ of the experimental runtime and the number of errors are a result of the high difficulty level of the task. Therefore, participants decided to follow various strategies, e. g. acting fast risking many errors or slow with probably a low number of errors.

The measured user force and torque vectors were normed and averaged over the experimental runtime (Table I, line no. 3 and line no. 4). The results in the table show significantly less user forces and torques for the VIC in relation to the PAC. The difference between the VIC+Obs. torques to the PAC torques is only a weak evidence. The comparison of VIC and VIC+Obs. show a significant difference of the user forces between these two settings. The values of the forces/torques of VIC+Obs. lie between both of these settings. Interestingly, the subjective experience of the participant measured by the question concerning the expenditure force (Table I, line no. 13) shows a different result. The participants experienced the VIC+Obs. to cause the lowest expenditure of force. In contrast to the objective measurement of the forces/torques of the VIC the participants recognized a large difference between the expenditure of force of the VIC and the PAC. We can only speculate for the reasons. Potentially, the participant experienced a smoother robot behavior due to the stability observer and interpreted this as a lower expenditure of force.

The measurements of the workload with the Raw NASA

TABLE I

RESULTS FOR THE PERFORMANCE DATA AND THE QUESTIONNAIRE OF THE USER STUDY.

			VIC+Obs.	t-test compare VIC+Obs. – PAC		**PAC**	t-test compare PAC – VIC		**VIC**	t-test compare VIC – VIC+Obs.	
no.		n	$\mu(\sigma)$	$\lvert t(0.975, n\text{-}1)\rvert$	p	$\mu(\sigma)$	$\lvert t(0.975, n\text{-}1)\rvert$	p	$\mu(\sigma)$	$\lvert t(0.975, n\text{-}1)\rvert$	p
1	Number of errors	45	10.1 (8.0)	0.175	0.862	9.9 (7.2)	0.419	0.677	9.4 (7.3)	0.519	0.606
2	Time in s	45	74.5 (29.9)	2.302	**0.013**	80.1 (34.7)	0.561	0.289	78.7 (38.5)	1.785	*0.081*
3	Mean of the norm of the user forces in N	40	9.54 (3.27)	1.362	0.181	9.91 (3.54)	2.847	**0.007**	9.04 (3.15)	2.238	**0.031**
4	Mean of the norm of the user torques in N m	40	1.49 (0.67)	1.909	*0.064*	1.61 (0.72)	3.337	**0.002**	1.38 (0.59)	1.913	*0.063*
5	Workload† in %	44	50.7 (12.0)	3.708	>**0.001**	59.5 (14.4)	1.323	0.193	56.4 (14.4)	2.376	**0.022**
6	Is functional*	45	3.6 (1.1)	2.238	**0.030**	3.1 (1.2)	0.955	0.345	3.3 (1.1)	2.141	**0.038**
7	Has a good force transmission*	45	3.7 (1.0)	3.572	>**0.001**	3.0 (1.3)	1.992	*0.053*	3.4 (1.2)	1.337	0.155
8	Has a nice-feeling handling*	45	3.4 (1.1)	2.030	**0.048**	3.0 (1.3)	0.545	0.588	3.1 (1.3)	1.522	0.135
9	Overall comfort*	44	3.5 (1.2)	2.332	**0.025**	3.0 (1.3)	1.336	0.189	3.3 (1.2)	1.341	0.135
10	How did you experience the user comfort of the robot (1: very bad) - (6: very good)	44	3.7 (1.2)	2.278	**0.028**	3.2 (1.4)	1.604	0.116	3.6 (1.2)	0.696	0.494
11	With the robot the task can be (1:very imprecise) - (6:very precise) performed	44	3.4 (1.2)	1.052	0.299	3.2 (1.2)	0.598	0.967	3.3 (1.3)	0.401	0.690
12	Where was your focus? (1: control the robot) - (6: carry out the task)	45	3.9 (1.6)	2.405	**0.020**	3.3 (1.6)	2.197	**0.033**	3.9 (1.5)	0.190	0.850
13	How do you rate the expenditure of force for the robot control? (1: very high) - (6: very low)	45	3.6 (1.4)	3.145	**0.003**	2.8 (1.4)	1.987	*0.053*	3.2 (1.3)	1.571	0.123
14	The robot behaves (1: very inert) - (6: very agile)	45	3.4 (1.4)	1.768	*0.084*	3.0 (1.3)	1.851	*0.071*	3.4 (1.2)	0.000	1.000

Legend: VIC – user force-dependent variable impedance controller, VIC+Obs. – VIC with an stability observer, PAC – pure admittance controlled robot, μ – mean, σ – standard deviation, n – samples, † [1], *[17]

TLX shows a significant improvement for the VIC+Obs. in relation to the PAC (Table I, line no. 5) which confirms our hypothesis. The improvement amounts to around 9 percent points. Contradicting our hypothesis, the workload of the VIC shows no significant difference to the workload of the PAC.

The results from the five questions of the CQH questionnaire (Table I, line no. 6 – 9) supports our hypothesis regarding user comfort for the VIC+Obs. in relation to the PAC. All these results shows significant improvements. Particularly, the question concerning the force transmission demonstrates an increase from 3.0 (PAC) to 3.7 (VIC+Obs.) which is an improvement of 14 percent points. In contrast to our expectations, the VIC shows no significant differences in relation to PAC. Only the question regarding force transmission results in a weak evidence for the difference between PAC and VIC. If there is an improvement of user comfort induced by VIC at all, then it is very small. The question regarding functionality is the only one which shows a significant difference between VIC and VIC+Obs.

Also, the direct question regarding user comfort (Table I, line no. 10) shows a significant improvement for the VIC+Obs. in relation to the PAC. This is typical for the validity of using the CQH questionnaire for analyzing user comfort of hand-guided robots. The user comfort of the VIC shows no significant difference to the comfort of the PAC. This also corresponds to the results of the CQH questionnaire.

Furthermore, we asked "Where was your focus?" (Table I, line no. 12). With both VIC types the focus of the participants was consequently more on the task than on controlling the robot in comparison to the PAC. This means with VIC and VIC+Obs., the hand-guided robot becomes a more efficient tool for the user.

We assumed that the participants would identify the VIC and the VIC+Obs. as more agile compared to the PAC. The results (Table I, line no. 14) show only a weak evidence and small differences between both types of VIC.

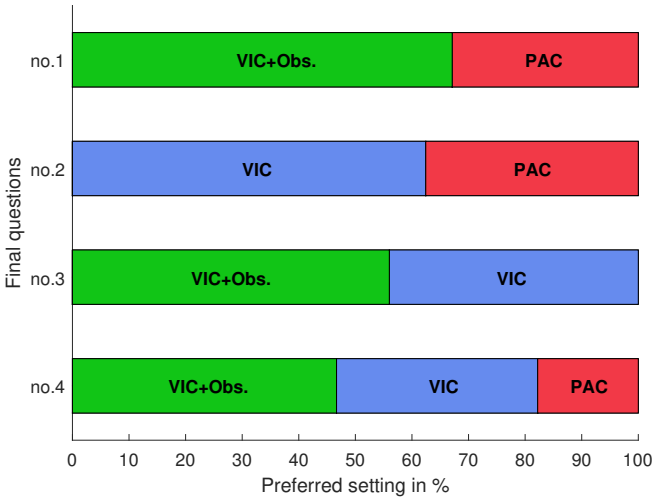


Fig. 5. Results for the final questionnaire with user force-dependent variable impedance controller (VIC), VIC with a stability observer (VIC+Obs.) and a pure admittance controlled robot (PAC).

Fig. 5 shows the results of the final questionnaire. The answers were sorted depending on the groups and the numbers (1-6) were converted into percentages. The first three results of the figure demonstrate the direct comparison between the separate trials. Both types of VIC are preferred over the PAC. The VIC+Obs. is only slightly more popular than the VIC. The final question (Fig. 5, no. 4) deals with the preferred trial. The graphical representation of the results show an obvious tendency to the VIC+Obs. Almost half of the participants decided for this type of controller. The PAC was the least favored controller in this study.

To summarize, the results show an improvement in using the VIC+Obs. for hand-guided robots in different aspects. With the VIC+Obs. a task with a hand-guided robot can

be solved faster and with the same accuracy compared to using a PAC. At least in the subjective experience, users need less expenditure of force. The workload and the user comfort are obviously smaller than using a PAC. The only advantage found in this study of the VIC over the VIC+Obs. is the lower need of user forces/torques. The used stability observer turned out to be an enhancement for the controller.

VI. Conclusion

In this paper we present a new type of variable impedance controller which is named user force-dependent variable impedance controller. This controller can be interpreted as a combination of a velocity dependent VIC and an acceleration dependent VIC. To guarantee the stability of the whole system, the controller was combined with a stability observer. This observer is based on a complex human model which consists of passive elements and delayed active behavior. Our implementation of the observer works like an additional user stiffness-dependent VIC. In a user study the VIC and the VIC+Obs. were compared to a pure admittance controller. In the study the participants guided the robot through a simple labyrinth. The VIC+Obs. was the most popular of the three investigated controllers of this study. Moreover, it was the controller with the lowest experimental runtime and had no significant difference in the number of errors. The users felt a lower expenditure of force, with lower workload and an improvement in user comfort.

In future works the force-dependent variable impedance control has to be compared in similar user studies to other types of variable impedance control as the velocity-dependent VIC or the acceleration-dependent VIC.

References

[1] J. C. Byers, A. C. Bittner, and S. G. Hill, "Traditional and raw task load index (tlx) correlations: Are paired comparisons necessary?" *Advances in Industrial Ergonomics and Safety. A. Mital (Ed.) Taylor & Francis*, pp. 481 – 485, 1989.

[2] J. E. Colgate and G. Schenkel, "Passivity of a class of sampled-data systems: application to haptic interfaces," *Journal of Robotic Systems*, vol. 14, no. 1, pp. 38–47, 1997.

[3] F. Dimeas and N. Aspragathos, "Learning optimal variable admittance control for rotational motion in human-robot co-manipulation," *11th IFAC Symposium on Robot Control (SYROCO)*, vol. 48, no. 19, pp. 124 – 129, Aug. 2015.

[4] V. Duchaine, B. Mayer-St-Onge, D. Gao, and C. Gosselin, "Stable and intuitive control of an intelligent assist device," *IEEE Transactions on Haptics*, vol. 5, no. 2, pp. 148–159, Apr. 2012.

[5] V. Duchaine and C. Gosselin, "Safe, stable and intuitive control for physical human-robot interaction," in *IEEE International Conference on Robotics and Automation (ICRA)*, 2009, pp. 3383–3388.

[6] ——, "General model of human-robot cooperation using a novel velocity based variable impedance control," in *EuroHaptics Conference, and Symposium on Haptic Interfaces for Virtual Environment and Teleoperator Systems. World Haptics. Second Joint*, Mar. 2007, pp. 446–451.

[7] ——, "Investigation of human-robot interaction stability using Lyapunov theory," in *IEEE International Conference on Robotics and Automation (ICRA)*, May 2008, pp. 2189–2194.

[8] M. S. Erden and A. Billard, "Robotic assistance by impedance compensation for hand movements while manual welding," *IEEE Transactions on Cybernetics*, vol. 46, no. 11, pp. 2459–2472, Nov. 2016.

[9] M. S. Erden and B. Marić, "Assisting manual welding with robot," *Robotics and Computer-Integrated Manufacturing*, vol. 27, no. 4, pp. 818 – 828, Aug. 2011.

[10] F. Ficuciello, L. Villani, and B. Siciliano, "Variable impedance control of redundant manipulators for intuitive human-robot physical interaction," *IEEE Transactions on Robotics*, vol. 31, no. 4, pp. 850–863, Aug. 2015.

[11] J. J. Gil, A. Avello, A. Rubio, and J. Florez, "Stability analysis of a 1 dof haptic interface using the routh-hurwitz criterion," *IEEE Transactions on Control Systems Technology*, vol. 12, no. 4, pp. 583–588, Jul. 2004.

[12] S. Grafakos, F. Dimeas, and N. Aspragathos, "Variable admittance control in phri using emg-based arm muscles co-activation," in *IEEE International Conference on Systems, Man, and Cybernetics (SMC)*, Oct. 2016, pp. 1900–1905.

[13] S. G. Hart, "Nasa-task load index (nasa-tlx); 20 years later," *Proceedings of Human Factors and Ergonomics Society Annual Meeting*, pp. 904– 908, Oct. 2006.

[14] N. Hogan, "Impedance control: An approach to manipulation: Part 1-3," *Journal of Dynamic Systems, Measurement, and Control*, vol. 107, pp. 1–24, Mar. 1985.

[15] R. Ikeura and H. Inooka, "Variable impedance control of a robot for cooperation with a human," in *IEEE International Conference on Robotics and Automation (ICRA)*, vol. 3, 1995, pp. 3097–3102.

[16] M. S. Khidiya and A. Bhardwaj, *Advances in Ergonomics Modeling and Usability Evaluation*. CRC Press, 2010, ch. Design of Hand Operated Trowel: An Ergonomic Approach, pp. 382–392.

[17] L. F. M. Kuijt-Evers, P. Vink, and M. P. de Looze, "Comfort predictors for different kinds of hand tools: Differences and similarities," *International Journal of Industrial Ergonomics*, vol. 37, pp. 73 – 84, 2007.

[18] A. Lecours, B. Mayer-St-Onge, and C. Gosselin, "Variable admittance control of a four-degree-of-freedom intelligent assist device," in *IEEE International Conference on Robotics and Automation (ICRA)*, May 2012, pp. 3903–3908.

[19] F. Müller, J. Jäkel and U. Thomas, "Stability analysis for a passive/active human model in physical human-robot interaction with multiple users," *submitted in International Journal of Control (preprint: http://kurzelinks.de/v8i4)*, Feb. 2018.

[20] F. Müller, J. Jäkel, U. Thomas and J. Suchý, "Stability of nonlinear time-delay systems describing human-robot interaction," *submitted with minor revision in IEEE/ASME Transactions on Mechatronics (preprint: http://kurzelinks.de/1o1y)*, 2018.

[21] K. Nishiwaki and K. Yano, "Variable impedance control of meal assistance robot using potential method," in *IEEE/RSJ International Conference on Intelligent Robots and Systems (IROS)*, Sep. 2008, pp. 3242–3247.

[22] N. Olgac and B. Holm-Hansen, "A novel active vibration absorption technique: Delayed resonator," *Journal of Sound and Vibration*, vol. 176, pp. 93–104, Sep. 1994.

[23] S. Sawilowsky and R. C. Blair, "A more realistic look at the robustness and type ii error probabilities of the test to departures from population normality," *Psychological Bulletin*, vol. 111, pp. 352–.360, Mar. 1992.

[24] M. R. Sirkin, *Statistics for the Social Science*. SAGE Publications, 1995.

[25] T. Tsumugiwa, R. Yokogawa, and K. Hara, "Variable impedance control based on estimation of human arm stiffness for human-robot cooperative calligraphic task," in *IEEE International Conference on Robotics and Automation (ICRA)*, vol. 1, 2002, pp. 644–650.

[26] ——, "Variable impedance control with virtual stiffness for human-robot cooperative peg-in-hole task," in *IEEE/RSJ International Conference on Intelligent Robots and Systems (IROS)*, vol. 2, Oct. 2002, pp. 1075–1081.

[27] T. Tsumugiwa, R. Yokogawa, and K. Yoshida, "Stability analysis for impedance control of robot for human-robot cooperative task system," in *IEEE/RSJ International Conference on Intelligent Robots and Systems (IROS)*, vol. 4, Sep. 2004, pp. 3883–3888.

[28] P. Vink and S. Hallbeck, "Editorial: Comfort and discomfort studies demonstrate the need for a new model," *Applied Ergonomics*, vol. 43, pp. 271–276, 2012.

[29] H. Wang, F. Patota, G. Buondonno, M. Haendl, A. De Luca, and K. Kosuge, "Stability and variable admittance control in the physical interaction with a mobile robot," *International Journal of Advanced Robotic Systems*, vol. 12, Dec. 2015.

[30] T. Yamawaki, H. Ishikawa, and M. Yashima, "Iterative learning of variable impedance control for human-robot cooperation," in *IEEE/RSJ International Conference on Intelligent Robots and Systems (IROS)*, Oct. 2016, pp. 839–844.